Subcellular Colocalization of Hypericin with Respect to Endoplasmic Reticulum and Golgi Apparatus in Glioblastoma Cells

RAINER RITZ[1], FLORIAN ROSER[1], NORBERT RADOMSKI[2], WOLFGANG S.L. STRAUSS[3], MARCOS TATAGIBA[1] and ALIREZA GHARABAGHI[1]

[1]*Department of Neurosurgery, Eberhard-Karls-Universität Tübingen;*
[2]*Olympus Soft Imaging Solutions, Münster;*
[3]*Institut für Lasertechnologien in der Medizin und Meßtechnik an der Universität Ulm, Ulm, Germany*

Abstract. *Background: To improve the poor prognosis of patients suffering from malignant glioma, hypericin (HYP)-based photodynamic therapy might be a promising approach. Intracellular localization of HYP was investigated by quantitative colocalization analysis with respect to endoplasmic reticulum (ER) and Golgi apparatus (GA) by double staining experiments with fluorescence microscopy. Materials and Methods: U373 MG glioblastoma cells were stained with HYP and costainings were applied for specific organelle markers for ER and GA. Results: In cells double-stained with HYP and ER-Tracker, 57% of HYP signals were found within the ER and 52% of the ER compartment showed HYP signals. The colocalization fraction of HYP found in the GA was 36% and 46% of the GA showed HYP signals. Conclusion: In glioblastoma cells, a considerable fraction of HYP is localized in the ER; in addition, a significant amount of the photosensitizer shows colocalization with the GA.*

Currently, standard treatment of glioblastoma is based on microsurgical tumour resection, radiation and chemotherapy (1). Overall prognosis of glioblastoma patients remains poor; therefore, new therapeutical options are necessary. Photodynamic therapy (PDT) of malignant glioma might be a promising treatment option in the future. PDT is based on the administration of a photosensitizer followed by exposure to light of the appropriate wavelength and the interaction of excited photosensitizer molecules with molecular oxygen. During illumination, reactive oxygen species (ROS) are generated which react with various biomolecules (*e.g.* proteins) inducing necrosis, apoptosis and autophagy (2, 3). Apoptosis, a fundamental mechanism in PDT, has been investigated at the morphological and biochemical levels (4). Intracellular organelles related to apoptosis in PDT are the endoplasmic reticulum (ER), lysosomes and mitochondria. The predominant localization of photosensitizers within cells varies significantly and depends on its physicochemical properties, *e.g.* lipophilicity (5-7). Hypericin (HYP), a lipophilic molecule produced by plants of the *Hypericum* genus, might be a promising substance for PDT of malignant glioma due to its efficient generation of ROS (8). The photodynamic properties of HYP in human glioblastoma cell lines have been reported (9, 10). An active transport mechanism for cellular HYP uptake has also been demonstrated; however, the subcellular distribution of HYP in glioblastoma cells has not been assessed (11). For a better understanding of HYP-mediated PDT, it will be of great importance to investigate the intracellular localization of HYP in more detail.

The purpose of the present study was to characterize the intracellular localization of HYP and quantify the colocalization patterns with ER and Golgi apparatus (GA).

Correspondence to: Dr. Rainer Ritz, Department of Neurosurgery, Eberhard-Karls-Universität Tübingen, Hoppe-Seyler-Straße 3, 72076 Tübingen, Germany. Tel: +49 7071 29 80325, Mobile: +49 173 3041231, e-mail: rainer.ritz@med.uni-tuebingen.de

Key Words: Hypericin, photodynamic therapy, glioma, intracellular localization, endoplasmatic reticulum, Golgi apparatus.

Materials and Methods

Cell culture. The human glioblastoma cell line U373 MG (ECACC No. 890811403) was obtained from the European Collection of Cell Cultures, Wiltshire, UK. The cell line was cultivated as described elsewhere (12). U373 MG cells were seeded at a defined density of 150 cells/mm^2 on glass slides (Nunc, Wiesbaden, Germany) 24 h prior to incubation. Golgi apparatus (GA) was stained with Lectin GS-II from *Griffonia simplicifolia* conjugated with Alexa Fluor™ 488 (Molecular Probes Europe BV, Leiden, The Netherlands) and was used at a concentration of 0.5 mg/ml for 20 min according to the manufacturer's protocol. Endoplasmic reticulum (ER) was labelled by ER-Tracker™ Green (glibenclamide BODIPY FL conjugate; Molecular Probes Europe BV), which was applied at a

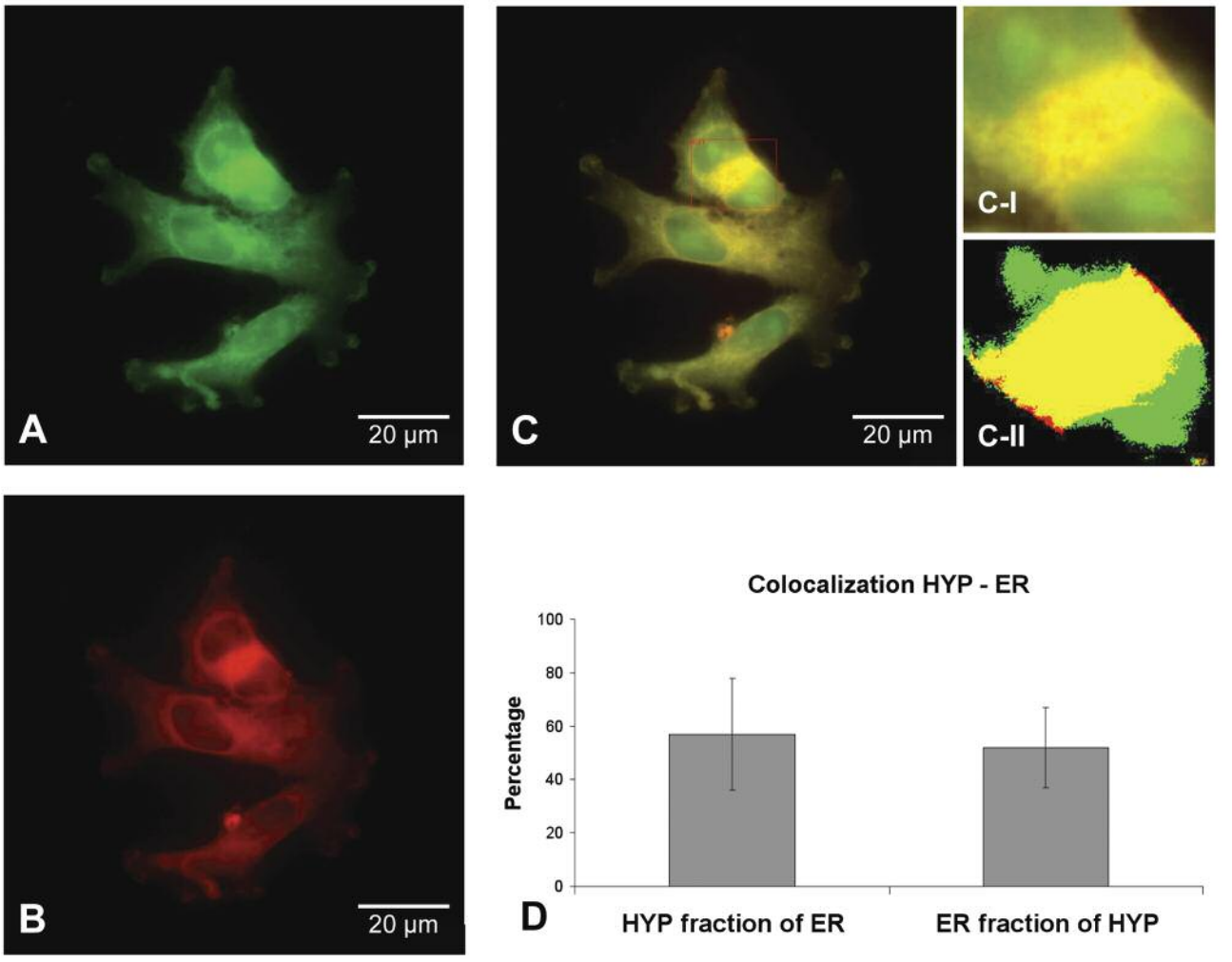

Figure 1. *Fluorescence microscopic images of U373 MG glioblastoma cells, co-stained with ER-Tracker (2 µM/20 min) and HYP (1 µM/2 h). The same cells visualized by U-MWBA3 filter (band-pass excitation filter 460-495 nm, band-pass emission filter 510-550 nm) for green fluorescence (ER) (A). U-MWG2 filter (band pass excitation filter 510-550 nm, long-pass emission filter 590 nm) for red fluorescence (HYP) (B). Superimposition and quantitative colocalization analysis is shown for a region of interest in (C), (C-I) original image, (C-II) after image processing. Magnification* ×*60, Olympus BX61 microscope, Hamburg, Germany. (D) Colocalization analysis ER-HYP: 57% ±21% (median±MAD) of HYP signals were found within the ER and 52% ±15% of the ER compartment showed a HYP signal; n=77.*

concentration of 2 µM for 20 min. After staining with one of the organelle markers, slides were washed twice with phosphate-buffered saline (PBS). Thereafter, samples were incubated with 1 µM HYP for 2 h. After washing again with PBS, cells were fixed by 3.7% paraformaldehyde for 10 min. Double stained ER-HYP and GA-HYP slides were covered with DAKO Cytomation fluorescence mounting medium (Dako, Hamburg, Germany). In all cases, at least three independent experiments were performed. Cultures incubated solely with one of the organelle markers served as controls.

Fluorescence microscopy. Fluorescence microscopy was carried out using an Olympus BX61 microscope (Olympus-Europa GmbH, Hamburg, Germany) equipped with a PLAPO60X (N.A. 1.4) oil immersion objective and filter sets for the detection of green fluorescence (U-MWBA3; excitation: 460-495 nm, emission: 510-550 nm) and red fluorescence (U-MWG2; excitation: 510-550 nm, emission: >590 nm). Images were obtained using an F-View II charge-coupled device camera (Olympus Soft Imaging Solutions GmbH, Münster, Germany). Images of single stained cells were acquired with both filters to determine possible cross-talks. Additionally, intensity measurements to determine the specific to non-specific ratio for the green fluorescence of both organelle markers and the red fluorescence of HYP were performed. Images of co-stained cells were analyzed with Cell^P software (Olympus Soft Imaging Solutions GmbH). Colocalization was determined applying a logical AND operation on two binary images derived from the original images of the green (organelle marker) and red channel (HYP) by appointing a specific intensity threshold in each

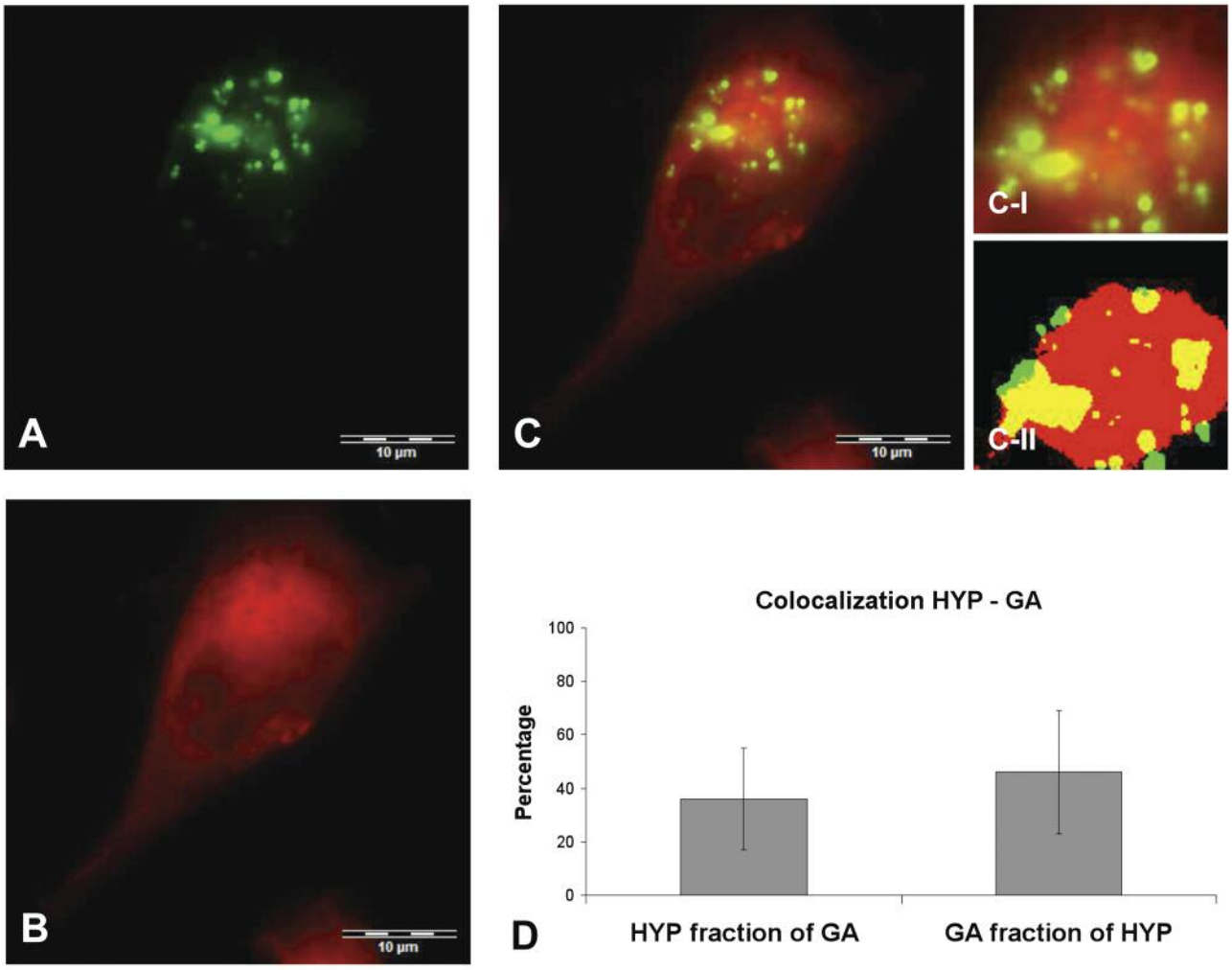

Figure 2. *Fluorescence microscopic images of U373 MG glioblastoma cells, co-stained with Golgi (0.5 mg/ml/20 min) and HYP (1 µM/2 h). Golgi apparatus was visualized by U-MWBA3 filter (band-pass excitation filter 460-495 nm, band-pass emission filter 510-550 nm) (A), HYP was visualized by U-MWG2 filter (band-pass excitation filter 510-550 nm, long-pass emission filter 590 nm) (B). Superimposition and quantitative colocalization analysis performed by software Cell^ P (C); (C-I) original image, (C-II) after image processing. Magnification* x60, *Olympus BX61 microscope, Hamburg, Germany. (D) Colocalization analysis Golgi-HYP: 36% ±19% (median±MAD) of HYP signals were found within the GA and 46% ±23% of the GA compartment showed a HYP signal; n=68.*

case. The quantitative analysis was calculated from n=77 fluorescence images for HYP-ER and n=68 fluorescence images for HYP-GA.

Results

Intracellular localization of HYP was investigated in U373 MG glioblastoma for a noncytotoxic incubation concentration of 1 µM (incubation time 2 h). At the beginning of three independent experiments, single stained cells were acquired with both filters to monitor possible cross-talks. No significant visible cross-talk was observed. Intensity measurements revealed a specific to non-specific ratio of 9.8 and 7.3 for green (organelle markers) and red fluorescence (HYP), respectively. Thus, fluorescence signals could be determined quite selectively with only minor cross-talk of below 15% in each case.

Micrographs of the U373 MG glioblastoma cells double-stained with HYP and ER Tracker Green are presented in Figure 1; cells double-stained with HYP and the GA marker are shown in Figure 2. HYP was mainly localized in the perinuclear region, irrespective of the applied organelle marker (Figure 1B / Figure 2B). Only weak fluorescence intensity was found in the nucleus.

The endoplasmic reticulum was predominantly found in the perinuclear region and exhibited a broad plane character

(Figure 1A). In contrast, the Golgi apparatus was found in a more granular pattern, even more distant from the nucleus (Figure 2A). Glioblastoma cells double-stained by HYP and ER-Tracker are given in Figure 1C as a superinposition of Figures 1A and 1B. Yellow areas correspond to areas of colocalization of HYP and ER-Tracker. Only weak fluorescence of HYP was seen in the nucleus. Colocalization in the cytoplasm with enrichment of both compounds in the perinuclear region was demonstrated quite nicely, as predictable from the staining patterns of each compound (Figure 1A and 1B).

Figure 2C demonstrates the glioblastoma cells double-stained by HYP and the GA marker. Again, yellow areas correspond to the colocalization fraction of HYP and the GA. The Golgi apparatus exhibited a granular fluorescence pattern mainly at the same site of the nucleus where HYP accumulation occured. For both colocalization experiments, regions of interest of the fluorescence images used for quantitative analysis are exemplarily shown prior to (Figures 1C-I and 2C-I) and after image processing (Figures1C-II and 2C-II).

In order to increase the significance of the co-staining experiments, fluorescence images were analyzed quantitatively and results are depicted in Figures 1D and 2D. In cells double-stained with HYP and ER marker, a median of 57% (±21%, median absolute deviation (MAD)) of HYP signals was found within the ER and 52%±15% (median±MAD) of the ER compartment showed HYP signals (Figure 1D). In the colocalization experiment, the colocalization fraction of HYP found in the GA was 36% (MAD 19%), whereas 46% (MAD 23%) of the GA coincided with the HYP fluorescence (Figure 2D).

Discussion

This study aimed at analysing the subcellular distribution of the lipophilic molecule HYP, a natural compound originating from plants of the genus *Hypericum*, in more detail. Commonly, HYP is found in the plant *Hypericum perforatum*, better known as St. John's wort. HYP, with its high triplet quantum yield, is a highly effective photosensitizer in malignant glioma (11). PDT is based on the reaction of singlet-oxygen with biomolecules. Due to their very short life-span, the cytotoxic species are only able to diffuse over short distances (10-20 nm). Considering cell sizes of approximately 20 μm, it is obvious that the subcellular localization of the photosensitizer becomes essential as the site of activity (13). As previously reported by several authors, HYP is enriched mainly in the perinuclear region, suggested as the ER (10, 12). To investigate HYP-mediated PDT in more detail, the intracellular distribution of these compounds with respect to the ER and GA was elucidated in a quantitative manner.

The ER consists of membrane-surrounded tubuli and cisterns extending from the nucleus into the cytoplasm. One main function of the ER is the processing and sorting of proteins. This is done in the so-called rough ER, which is enriched by ribosomes on the outer membrane, mainly producing proteins. From the rough ER, the smooth ER is distinguished. The smooth ER is the major site at which membrane lipids are synthesized. The GA, consisting of cisternae and associated vesicules, is in close vicinity to the ER.

The proteins received from the ER are processed and sorted in the GA for their further application. Additionally, the GA has also important functions in lipid metabolism. In particular, glycolipids and sphingomyelins are synthesized in this cell organelle. GA and ER are in a close morphological and dynamic functional relationship, while there is a continuous cycling between the two cell organelles (14-16).

PDT requires a photosensitizer, light of appropriate wavelength and molecular oxygen to generate ROS. Oxidative damage of lipids, proteins and nucleic acids leads to cell death by several pathways. Apoptosis is a fundamental mechanism of cell death. Intracellular organelles, *e.g.* mitochondria, lysosomes and the ER, are involved in apoptosis. Ca^{2+} homeostasis and shifts in Ca^{2+} compartmentalization play an important role in triggering apoptosis (17). In the case of the photosenitizer verteprofin, a derivative of benzoporphyrine, PDT results in the release of Ca^{2+} from the ER and mitochondria, which plays a major role in apoptosis (18). Recently, deregulated ER-Ca^{2+} homeostasis after HYP-PDT was reported (19). Based on these data, the present data on the subcellular distribution of HYP may contribute to a better understanding of HYP-mediated PDT.

Golgi apparatus has important functions in lipid metabolism. Therefore, a high affinity of HYP, a lipophilic compound, to the GA was supposed and investigated. To date, only minor endeavour has been made to investigate the relation between damage of the GA and PDT, particularly in the case of HYP-mediated PDT. Subcellular localization as well as mechanisms of PDT varies for different photosensitizers. HPD (Photofrin™), a first-generation photosensitizer composed of a complex mixture of porphyrins, was first applied by Lipson and Schwarz in 1960. Mitochondrial localization was demonstrated in radiation-induced double-labelled fibrosarcoma tumor cells by confocal fluorescence microscopy (20). The data concerning the subcellular localization of Photofrin™ differ. Hsieh *et al.* demonstrated a very high colocalization of Photofrin™ and GA complex by selective fluorescence staining with BODOPY FL C5-ceramide for long incubation times and plasma membranes after short incubation times (6).

Second-generation sensitizers such as phthalocyanines and chlorines are typically located in the cytoplasm. More detailed information about intracellular location exists for

Foscan™ (*meso*-tetra(*m*-hydroxyphenyl)chlorin, *m*-THPC), a second-generation photosensitizer. It was localized in ER and GA as demonstrated by Teiten *et al*. and Marchal *et al*. (21, 22). Teiten *et al*. evaluated enzymatic activities after photosensitizing MCF-7 cells (human breast cancer cells) with Foscan™ and demonstrated that uridine 5'-diphosphate galactosyl transferase, an enzyme located in the GA, was inactivated after PDT (21). Marchal *et al*. demonstrated good colocalization of *m*-THPC with the GA after an incubation time of 3 hours. The authors found only weak correlation to a mitochondrial marker. In contrast, Yow *et al*. demonstrated in the nasopharyngeal carcinoma cell line NPS/HK1 that most mitochondria were targeted by *m*-THPC (7). These authors found a similar intracellular localization pattern with respect to mitochondria for HPD and *m*-THPC.

Chiu *et al*. showed a high release of cytochrome *c* from mitochondria by PDT with phthalocyanine 4, suggesting that the PDT-induced cell death by apoptosis mainly correlates with the release of cytochrome *c* from mitochondria (5). Chen *et al*. demonstrated the mitochondrion as an important cell organelle in PDT-mediated apoptosis by merocyanine 540 in murine myeloid leukaemia (JCS) cells by confocal laser scanning microscopy (23). Lysosomes have been shown as a potential site of hydrophilic sensitizers in PDT, *e.g*. tetraphenylporphyrins, or Nile blue derivatives (24-27).

A modern fluorescence marker (and photosensitizer), well established in neurosurgery for visualisation of malignant glioma, is protoporphyrin IX (PP IX). Accumulation of PP IX in malignant cells occurs after administration of the pro-drug 5-aminolevulinic acid (5-ALA) (28), possibly based on a diminished activity of ferrochelatase, one of the key enzymes of heme-biosynthesis. Recently, in a fluorescence microscopic study, Ji *et al*. revealed that 5-ALA-induced PP IX was mainly located in mitochondria (29). Similar results were obtained by investigating subcellular colocalization analysis of Photofrin™ and PP IX with mitochondria-specific markers by confocal fluorescence microscopy (20). The photosensitizer used in the present study was HYP, a strongly hydrophobic compound. As reported previously by our group, HYP showed a quite different fluorescence pattern as compared to lysosomes and mitochondria, stained by acridine orange and rhodamine 123, respectively (11). The present study reveals both descriptively and quantitatively the subcellular distribution of HYP in human glioma cells by fluorescence microscopy. In order to gain reliable results, the selection of the appropriate filter sets is quite crucial. Due to the broad fluorescence emission above 600 nm, the green fluorescence of the organelle marker was detected with a band-pass emission filter for 510-550 nm. Thus, a significant reduction of fluorescence cross-talk was found as compared to a standard filter set (long-pass emission filter), which improved our results considerably (data not shown).

In conclusion, the present data suggest that the ER seems to be an important target of HYP-mediated PDT. In addition, damage to the GA might also be involved in PDT-induced cell death; however the colocalization data indicate that its contribution seems to be of minor importance as compared to ER damage. These data may lead to a better appreciation of new approaches of PDT in the therapy of malignant glioma. For the future it will be of great interest to find concepts for improving efficacy of HYP-PDT, *e.g*. by increasing the photosensitization of malignant cells.

Acknowledgements

The authors appreciate the technical assistance by A. Gruber, Department of Neurosurgery, University Hospital Tübingen, Germany.

References

1 Stupp R, Mason WP, van den Bent MJ, Weller M, Fisher B, Taphoorn MJ, Belanger K, Brandes AA, Marosi C, Bogdahn U, Curschmann J, Janzer RC, Ludwin SK, Gorlia T, Allgeier A, Lacombe D, Cairncross JG, Eisenhauer E and Mirimanoff RO: Radiotherapy plus concomitant and adjuvant temozolomide for glioblastoma. N Engl J Med *352*: 987-996, 2005.

2 Dougherty TJ, Gomer CJ, Henderson BW, Jori G, Kessel D, Korbelik M, Moan J and Peng Q: Photodynamic therapy. J Natl Cancer Inst *90*: 889-905, 1998.

3 Vrouenraets MB, Visser GW, Snow GB and van Dongen GA: Basic principles, applications in oncology and improved selectivity of photodynamic therapy. Anticancer Res *23*: 505-522, 2003.

4 Kessel D, Vicente MG and Reiners JJ Jr: Initiation of apoptosis and autophagy by photodynamic therapy. Lasers Surg Med *38*: 482-488, 2006.

5 Chiu S, Evans HH, Lam M, Nieminen A and Oleinick NL: Phthalocyanine 4 photodynamic therapy-induced apoptosis of mouse L5178Y-R cells results from a delayed but extensive release of cytochrome *c* from mitochondria. Cancer Lett *165*: 51-58, 2001.

6 Hsieh YJ, Wu CC, Chang CJ and Yu JS: Subcellular localization of Photofrin™ determines the death phenotype of human epidermoid carcinoma A431 cells triggered by photodynamic therapy when plasma membranes are the main targets. J Cell Physiol *194*: 363-375, 2003.

7 Yow CM, Chen JY, Mak NK, Cheung NH and Leung AW: Cellular uptake, subcellular localization and photodamaging effect of temoporfin (mTHPC) in nasopharyngeal carcinoma cells: comparison with hematoporphyrin derivative. Cancer Lett *157*: 123-131, 2000.

8 Diwu Z and Lown JW: Photosensitization with anticancer agents. 17. EPR studies of photodynamic action of hypericin: formation of semiquinone radical and activated oxygen species on illumination. Free Radic Biol Med *14*: 209-215, 1993.

9 Couldwell WT, Gopalakrishna R, Hinton DR, He S, Weiss MH, Law RE, Apuzzo ML and Law RE: Hypericin: a potential antiglioma therapy. Neurosurgery *35*: 705-709, 1994.

10 Uzdensky AB, Ma LW, Iani V, Hjortland GO, Steen HB and Moan J: Intracellular localisation of hypericin in human glioblastoma and carcinoma cell lines. Lasers Med Sci *16*: 276-283, 2001.

11 Ritz R, Wein HT, Dietz K, Schenk M, Roser F, Tatagiba M and Strauss WS: Photodynamic therapy of malignant glioma with hypericin: comprehensive *in vitro* study in human glioblastoma cell lines. Int J Oncol *30*: 659-667, 2007.
12 Ritz R, Muller M, Weller M, Dietz K, Kuci S, Roser F and Tatagiba M: Hypericin: a promising fluorescence marker for differentiating between glioblastoma and neurons *in vitro*. Int J Oncol *27*: 1543-1549, 2005.
13 Moan J and Berg K: The photodegradation of porphyrins in cells can be used to estimate the lifetime of singlet oxygen. Photochem Photobiol *53*: 549-553, 1991.
14 Rhee SW, Starr T, Forsten-Williams K and Storrie B: The steady-state distribution of glycosyltransferases between the Golgi apparatus and the endoplasmic reticulum is approximately 90:10. Traffic *6*: 978-990, 2005.
15 Storrie B: Maintenance of Golgi apparatus structure in the face of continuous protein recycling to the endoplasmic reticulum: making ends meet. Int Rev Cytol *244*: 69-94, 2005.
16 Cooper G: Cell structure and function. *In*: The Cell. A Molecular Approach. Cooper GM (ed.). www.ncbi.nlm.nih.gov/books/bv.fcgi?rid=cooper. 2000.
17 Orrenius S, Zhivotovsky B and Nicotera P: Regulation of cell death: the calcium-apoptosis link. Nat Rev Mol Cell Biol *4*: 552-565, 2003.
18 Granville DJ, Ruehlmann DO, Choy JC, Cassidy BA, Hunt DW, van Breemen C and McManus BM: Bcl-2 increases emptying of endoplasmic reticulum Ca^{2+} stores during photodynamic therapy-induced apoptosis. Cell Calcium *30*: 343-350, 2001.
19 Buytaert E, Callewaert G, Hendrickx N, Scorrano L, Hartmann D, Missiaen L, Vandenheede JR, Heirman I, Grooten J and Agostinis P: Role of endoplasmic reticulum depletion and multidomain proapoptotic BAX and BAK proteins in shaping cell death after hypericin-mediated photodynamic therapy. FASEB J *20*: 756-758, 2006.
20 Wilson BC, Olivo M and Singh G: Subcellular localization of Photofrin™ and aminolevulinic acid and photodynamic cross-resistance *in vitro* in radiation-induced fibrosarcoma cells sensitive or resistant to Photofrin-mediated photodynamic therapy. Photochem Photobiol *65*: 166-176, 1997.
21 Teiten MH, Marchal S, D'Hallewin MA, Guillemin F and Bezdetnaya L: Primary photodamage sites and mitochondrial events after Foscan photosensitization of MCF-7 human breast cancer cells. Photochem Photobiol *78*: 9-14, 2003.
22 Marchal S, Francois A, Dumas D, Guillemin F and Bezdetnaya L: Relationship between subcellular localisation of Foscan and caspase activation in photosensitised MCF-7 cells. Br J Cancer *96*: 944-951, 2007.
23 Chen JY, Cheung NH, Fung MC, Wen JM, Leung WN and Mak NK: Subcellular localization of merocyanine 540 (MC540) and induction of apoptosis in murine myeloid leukemia cells. Photochem Photobiol *72*: 114-120, 2000.
24 Berg K and Moan J: Lysosomes and microtubules as targets for photochemotherapy of cancer. Photochem Photobiol *65*: 403-409, 1997.
25 Geze M, Morliere P, Maziere JC, Smith KM and Santus R: Lysosomes, a key target of hydrophobic photosensitizers proposed for photochemotherapeutic applications. J Photochem Photobiol B *20*: 23-35, 1993.
26 Lin CW, Shulok JR, Kirley SD, Cincotta L and Foley JW: Lysosomal localization and mechanism of uptake of Nile blue photosensitizers in tumor cells. Cancer Res *51*: 2710-2719, 1991.
27 Wessels JM, Strauss W, Seidlitz HK, Ruck A and Schneckenburger H: Intracellular localization of *meso*-tetraphenylporphine tetrasulphonate probed by time-resolved and microscopic fluorescence spectroscopy. J Photochem Photobiol B *12*: 275-284, 1992.
28 Stummer W, Pichlmeier U, Meinel T, Wiestler OD, Zanella F and Reulen HJ: Fluorescence-guided surgery with 5-aminolevulinic acid for resection of malignant glioma: a randomised controlled multicentre phase III trial. Lancet Oncol *7*: 392-401, 2006.
29 Ji Z, Yang G, Vasovic V, Cunderlikova B, Suo Z, Nesland JM and Peng Q: Subcellular localization pattern of protoporphyrin IX is an important determinant for its photodynamic efficiency of human carcinoma and normal cell lines. J Photochem Photobiol B *84*: 213-220, 2006.

Received February 20, 2008
Revised May 14, 2008
Accepted May 15, 2008